

OBSERVATIONS OF GAMMA-RAY EMISSION FROM THE BLAZAR MARKARIAN 421 ABOVE 250 GeV WITH THE CAT CHERENKOV IMAGING TELESCOPE

F. Piron¹, for the CAT collaboration

¹LPNHE, Ecole Polytechnique and IN2P3/CNRS, Palaiseau, France

Abstract

The γ -ray emission of the blazar Markarian 421 above 250 GeV has been observed by the CAT Cherenkov imaging telescope since December, 1996. We report here results on the source variability up to April, 1998, with emphasis on the 1998 campaign. For the flaring periods of this year, the energy spectrum was derived from 330 GeV up to 5.2 TeV: it is very well represented by a simple power law, with a differential spectral index of 2.96 ± 0.13 .

1 Introduction

Markarian 421 (Mrk 421) is one of the three extragalactic sources detected to date from the Northern hemisphere at TeV energies, along with Markarian 501 and 1ES2344. In particular, it is the closest BL Lac object ($z = 0.030$), as well as the first one discovered in the very high energy (VHE) range: shortly after its detection between 50 MeV and a few GeV by the EGRET instrument on board the *Compton Gamma Ray Observatory* (Lin, et al. 1992), the Whipple group observed it at a 6.3σ level at TeV energies (Punch, et al. 1992). Since then, it has remained one of the most studied blazars, and was the object of several multi-wavelength observation campaigns (see, e.g., Macomb, et al. 1995, and Takahashi, et al. 1996).

Since it started operation in Autumn

1996, the CAT (Cherenkov Array at Thémis) telescope has been observing Mrk 421 regularly. The next section describes briefly the detector and the analysis method used to extract the signal. Then, the Mrk 421 data sample and the corresponding light curve up to April 1998 are presented in Sect. 3. Finally, the spectral properties observed in 1998 are examined in Sect. 4, and a discussion is given in Sect. 5.

2 The CAT detector: characteristics and analysis method

The most complete descriptions of the CAT experiment and of its specific analysis method can be found in (Barrau, et al. 1998) and (Le Bohec, et al. 1998), respectively. We just recall here the few characteristics which are necessary for the understanding of the following sections.

Located on the site of the former solar plant Thémis (French Pyrénées), the CAT detector uses the now-

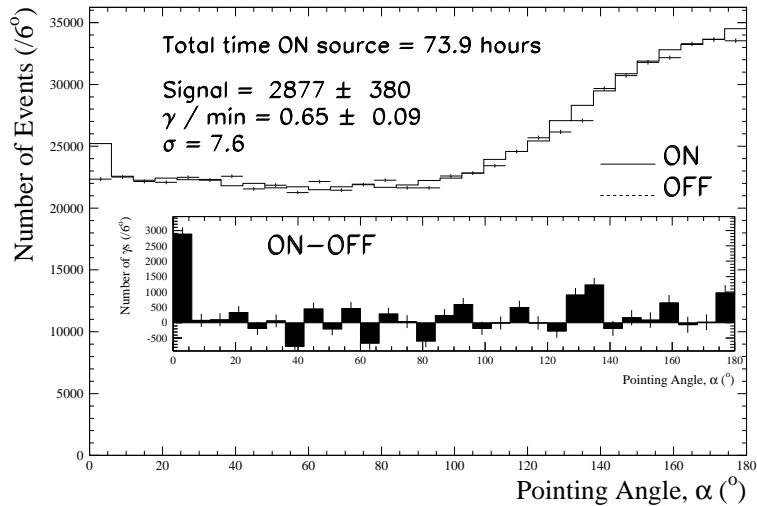


Figure 1: Distribution of the pointing angle α (see Sect. 2 for definition) of Mrk 421 for all data between December 1996 and April 1998. The signal is clearly seen in the first bin.

validated technique of Cherenkov imaging. The Cherenkov light emitted by the secondary particles produced during the development of atmospheric showers is collected through a large mirror which forms their image in its focal plane. The CAT camera, placed 6 m from its 4.7 m diameter mirror, has a 4.8° full field of view, which is comprised of a central region of $546 \times 0.12^\circ$ angular diameter phototubes in a hexagonal matrix and of 54 surrounding tubes in two “guard rings”. Its very high definition, combined with fast electronics, is an efficient solution of the two main problems one has to face with such γ -ray detectors: firstly, the detection threshold, which is determined by the night-sky background, is relatively low (250 GeV at Zenith); secondly, the capability of rejecting the enormous cosmic-ray background (protons, nuclei) is improved by an accurate analysis based on the comparison of individual images with theoretical mean γ -ray images, i.e. by the fit of an analytical model which uses the whole information contained in the images’ longitudinal light profile. This fit allows the direction and energy of γ -ray events to be determined with good accuracy, with an angular resolution per event of the order of the pixel size, and an energy resolution about 20% (independent of energy) when selecting showers with an impact parameter less than 130 m. Two main cuts are needed for the γ -ray selection. After keeping the highest-energy triggers (total charge $Q_{\text{tot}} > 30$ photo-electrons), a first cut on the probability given by the fit $P(\chi^2) > 0.35$ is applied, which selects the images with a “ γ -like” shape. Since γ -ray images are expected to point towards the source position in the camera, a second cut $\alpha < 6^\circ$ is used, where the pointing angle α is defined as the angle at the image barycentre between the actual source position and the reconstructed angular origin of the image. As a result, this procedure rejects 99.5% of hadronic events while keeping 40% of γ -ray events. A source like the Crab nebula, which is generally considered as the standard candle for γ -ray astronomy, can be detected at a 4.5σ level in one hour and localised within 1 to 2 arcmin.

3 Data sample

The γ -ray emission of Mrk 421 above 250 GeV has been observed by CAT from December 1996 onwards. Here we consider data taken up to April 1998. A selection based on criteria requiring clear weather and stable detector operation has been applied. This leaves a total of 73.9 hours of on-source (ON) data, together with 33 hours on control (OFF) regions, for a zenith angle band extending up to 40° . Fig. 1 shows the distribution of the pointing angle α for the whole sample. With the cuts quoted in Sect. 2, the mean γ -rate is found to be of the order of one third of that of the Crab nebula, with a total significance reaching the 7.6σ level. After Mrk 501, this makes Mrk 421 the second extragalactic source detected by CAT.

As can be seen on Fig. 2, the emission of Mrk 421 changed significantly between 1996-97 and

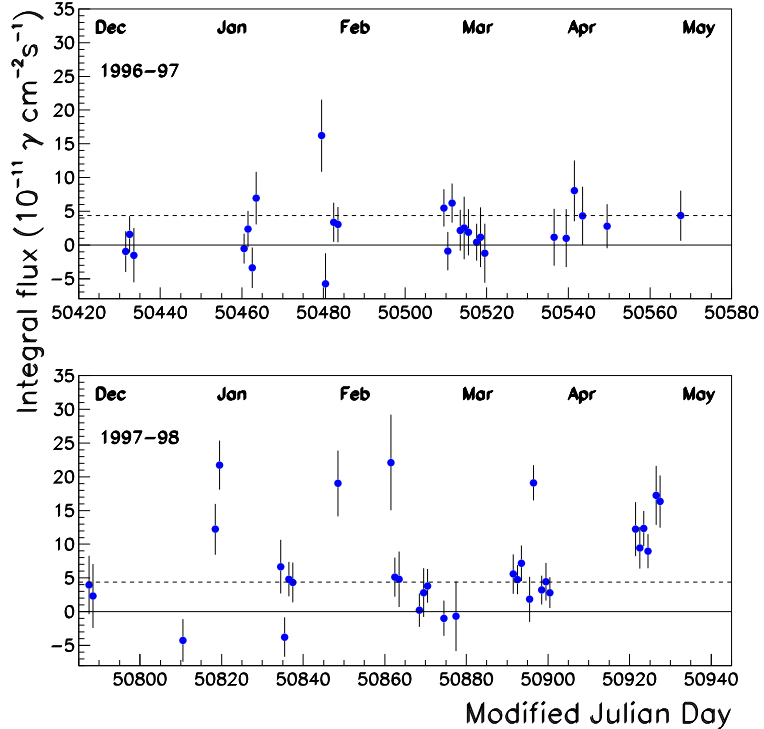


Figure 2: Mrk 421 nightly integral flux levels above 250 GeV, for observations between December 1996 and April 1998. The spectral shape as derived in Sect. 4 has been assumed to estimate the integral flux for observations far from the Zenith. The dashed line represents the mean flux over the two years.

1997-98: almost quiet in the first period (with a mean integral flux $\phi(> 250 \text{ GeV}) = 1.94 \pm 0.65 \times 10^{-11} \text{ cm}^{-2} \text{ s}^{-1}$), the source showed small bursts in the second period, together with a higher mean activity ($\phi(> 250 \text{ GeV}) = 6.05 \pm 0.54 \times 10^{-11} \text{ cm}^{-2} \text{ s}^{-1}$). Fig. 3 is a zoom on the small flare of the night between 24 and 25 March, 1998, which reached a maximum of ~ 2 times the Crab emission level. Three days after this flare, a VLBI observation showed a strong decrease of the radio emission polarization and intensity from the core of the galactic nucleus (Charlot, et al. 1999), in comparison with a first measurement performed three weeks earlier. The insufficient time-coverage between the radio and TeV observations unfortunately precludes any further interpretation.

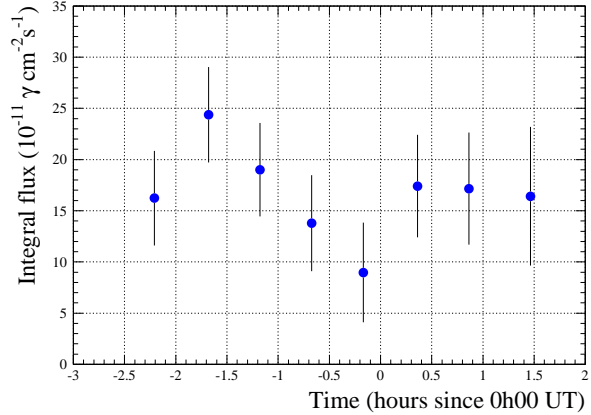


Figure 3: Light curve of the night between 24 and 25 March, 1998 (MJD 50896/50897). Each point represents a run of ~ 30 min.

4 Mrk 421 spectrum in 1998

A spectrum was derived for the flaring periods of Mrk 421 in 1998. The data used in this section have been further limited to zenith angles $< 16^\circ$, i.e. to a configuration for which the detector calibration has been fully completed. By minimizing systematic effects, this allows a robust spectral determination. Another favourable factor is the low night-sky background in the field of view, due to the lack of bright stars around the source.

The spectrum was derived in two steps: firstly, the number of events for each energy and zenith angle bin within the cuts quoted in Sect. 2 was determined for ON and OFF runs; secondly, taking into account the trigger and cut efficiencies as well as the energy resolution of the telescope, a maximum likelihood estimation of the spectral parameters has been applied for the simple power law hypothesis (\mathcal{H}_0) $d\Phi/dE_{\text{TeV}} = \phi_0 E_{\text{TeV}}^{-\gamma}$. As can be seen in Fig. 4, this accounts very well for the observed spectrum between 330 GeV and 5.2 TeV, which was the energy range considered. With a correlation coefficient of -0.68 , the fitted parameters are:

$$\phi_0 = 1.96 \pm 0.20^{\text{stat}} \pm 0.12^{\text{sys-MC}} \times 10^{-11} \text{ cm}^{-2} \text{ s}^{-1} \text{ TeV}^{-1} \text{ and}$$

$$\gamma = 2.96 \pm 0.13^{\text{stat}} \pm 0.05^{\text{sys-MC}}.$$

Systematics errors due to limited Monte Carlo statistics (noted “sys-MC”) in the determination of the effective detection area affect both ϕ_0 and γ . The second systematics errors (noted “sys-atm”) come from the uncer-

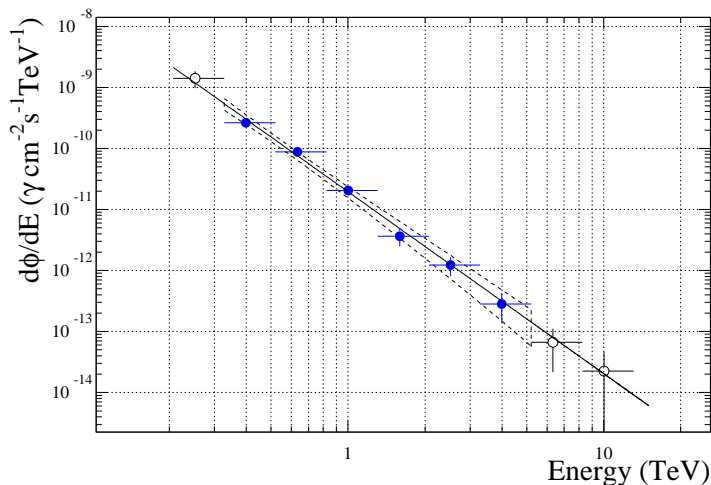


Figure 4: Differential flux of Mrk 421 for the flaring periods in 1998. Individual intensities per bin are only indicative and the error bars are statistical. The full line represents the power law parameters estimated by a likelihood method, in which only the fulfilled circles were used (see text). This method gives also the 2σ error “box”, whose shape reflects the correlation between the parameters. This latter vanishes at the decorrelation energy $E_d = 580 \text{ GeV}$.

tainty on the absolute energy scale. They are due to variations of the transparency of the atmosphere and affect only the absolute flux.

5 Discussion

The spectral shape of Mrk 421 observed by CAT in 1998 is fully compatible with recent results from the HEGRA collaboration (Aharonian, et al. 1999). It is however in contrast with the former behaviour of the source at the time of the 1995 and 1996 flaring periods, as observed by the Whipple group, who found $\gamma = 2.54 \pm 0.03^{\text{stat}} \pm 0.10^{\text{sys}}$ (Krennrich, et al. 1999). The higher value of the differential spectral index found here thus seems to favour a correlation between the intensity level and the spectral shape. Actually, such a correlation has been recently reported by CAT on the extreme blazar Mrk 501 (Djannati-Ataï, et al. 1999; see also Tavernet, et al. 1999). Since the spectrum of the latter is now known to be curved for very intense emissions, the hypothesis (\mathcal{H}_1) of a curved shape $d\Phi/dE_{\text{TeV}} = \phi_0 E_{\text{TeV}}^{-(\gamma+\beta \log_{10} E_{\text{TeV}})}$ was also considered for Mrk 421. The fitted curvature term is $\beta = 0.28 \pm 0.49$, compatible with zero. The likelihood ratio $\lambda = -2 \times \log \frac{\mathcal{L}(\mathcal{H}_0)}{\mathcal{L}(\mathcal{H}_1)}$, which gives an estimate of the relevance of \mathcal{H}_1 with respect to \mathcal{H}_0 and behaves asymptotically like a χ^2 with one d.o.f., is 0.34, corresponding to a chance probability of 0.56. This confirms the absence of any obvious spectral curvature for Mrk 421, as already indicated by Krennrich, et al. 1999. In the framework of leptonic models (Ghisellini, et al 1998), which succesfully explain the Mrk 501 spectral energy distribution in the X-ray and VHE γ -ray ranges (Djannati-Ataï, et al. 1999), the present result implies that the peak energy of the inverse Compton contribution of Mrk 421 is significantly lower than the CAT detection threshold. This is not surprising since the corresponding synchrotron peak is lower than that of Mrk 501, and since leptonic models predict a strong correlation between X-rays and γ -rays. Moreover, such a correlation was directly observed on Mrk 421 in Spring 1998, during a coordinated observation campaign involving ground-based Cherenkov imaging telescopes (Whipple, HEGRA, and CAT) and the ASCA X-ray satellite (Takahashi, et al. 1999).

References

- Aharonian, F.A., et al. 1999, submitted to A&A
- Barrau, A., et al. 1998, Nucl. Instr. Meth. A416, 278
- Charlot, P., et al. 1999, Proc. 19th Texas Symposium, Paris 1998, in press
- Djannati-Ataï, A., et al. 1999, submitted to A&A
- Ghisellini, G., et al. 1998, MNRAS 301, 451
- Krennrich, F., et al. 1996, ApJ 481, 758
- Krennrich, F., et al. 1999, ApJ 511, 149
- Le Bohec, S., et al. 1998, Nucl. Instr. Meth. A416, 425
- Lin, Y.C., et al. 1992, ApJ 401, L61
- Macomb, D.J., et al. 1995, ApJ 449, L99
- Punch, M., et al. 1992, Nature 358, 477
- Takahashi, T., et al. 1996, ApJ 470, L89
- Takahashi, T., et al. 1999, to be published
- Tavernet, J.-P., et al. 1999, this Proc., OG 2.1.08